Available online at www.sciencedirect.com
SCIENCE DIRECT®
Journal of Electroanalytical Chemistry 540 (2003) 45–52
Journal of Electroanalytical Chemistry
www.elsevier.com/locate/jelechem

Self-assembly of (3-mercaptopropyl)trimethoxysilane on iodine coated gold electrodes

D.R. Blasini [a], R.J. Tremont [a], N. Batina [b], I. González [b], C.R. Cabrera [a,*]

[a] Department of Chemistry, University of Puerto Rico, Río Piedras Campus, P.O. Box 23346, San Juan, PR 00931-3346, USA
[b] Departamento de Química, Universidad Autónoma Metropolitana Iztapalapa, Apartado Postal 55-534, Mexico 09340, Mexico

Received 11 December 2001; received in revised form 10 September 2002; accepted 22 October 2002

Abstract

The adsorption of (3-mercaptopropyl)trimethoxysilane (MPS) has been studied on iodine coated gold electrodes. The MPS adsorption from alcoholic solution on Au(111) and iodine coated Au(111) was studied by atomic force microscopy (AFM) and X-ray photoelectron spectroscopy (XPS). The electrochemical formation of MPS monolayers was studied by cyclic voltammetry on polycrystalline uncoated and coated gold electrodes with different MPS pre-treatment conditions. Lead electrochemical deposition was used to probe the defect sites of the surfaces created. The MPS-over-iodine coated gold surface produces a lower-density monolayer than the MPS over pure gold. The MPS monolayer formed electrochemically on the iodine coated gold is chemically equal to its counterpart after the iodine desorption. The MPS adsorption occurs via an Au–S bond, after the partial reductive-desorption of the iodine monolayer from the iodine coated gold electrode, and produces an ordered composite monolayer of MPS/iodine. The size of the defects can be controlled by varying the electrochemical preparation conditions, using the following reaction: $Au\text{–}I_{(ads)} + MPS\text{–}H_{(ac)} + e^- \leftrightarrow Au\text{–}MPS_{(ads)} + H^+_{(ac)} + I^-_{(ac)}$.

Keywords: Self-assembled monolayers; 3-Mercaptopropyltrimethoxysilane; Gold

1. Introduction

The preparation of highly-ordered monolayers by molecular self-assembly has been employed extensively as a surface derivatization procedure. This method has a wide use in the preparation of modified surfaces [1–4]. Many of these highly ordered monolayer systems find application in the areas of catalysis, electron transfer kinetics, lithography, electronics devices, lubrication and wetting [5–9]. The self-assembly phenomena allow the easy preparation of modified electrodes with high degrees of structural order [10–19]. The formation of high-order monolayers is often done by the spontaneous adsorption of *n*-alkanethiols or their derivatives to gold surfaces [20,21]. Another way to prepare these *n*-alkanethiols monolayers is by electrochemical adsorption/desorption by the following reaction [22–25]:

$$AuS(CH_2)_n\ X + e^- \rightarrow Au + X(CH_2)_n\ S^- \quad (1)$$

Reaction (1) can be employed to control the defect sizes of the monolayer and use the modified electrode as a molecular recognition device [26–28].

An alternative route to the formation of highly ordered molecular arrays via self-ordering is employing iodine-modified Au(111) electrodes for the adsorption of organic molecules, such as TMPyP, crystal violet (CV) and PPV [29,30]. It was clarified that the iodine adlayer on these iodine-modified electrodes played a crucial role on the formation of highly ordered molecular arrays. The key factor promoting the self-ordering is the relatively weak van der Waals type interactions between the hydrophobic iodine adlayer and the organic molecules. It is well known that chemisorption of aqueous iodine onto gold occurs oxidatively by forming a monolayer of zero-valent iodine species on the surface [31]. Iodine adlayers on Au(111) have been characterized by using scanning tunneling microscopy (STM) in air, in situ STM, low-energy electron diffraction (LEED), and surface X-ray scattering (SXS) techniques [32–36]. Two

* Corresponding author. Tel.: +1-787-764-0000x4807; fax: +1-787-756-8242.
E-mail address: ccabrera@cnnet.clu.edu (C.R. Cabrera).

0022-0728/02/$ - see front matter © 2002 Elsevier Science B.V. All rights reserved.
PII: S0022-0728(02)01275-5

distinct incommensurate iodine monolayer phases have been observed. In both of them the structures compress with increasing potential. This phenomenon is called electrocompression [36]. In the lower potential phase a ($p \times \sqrt{3}$) centered-rectangular iodine has been reported in which the coverage (θ) increases from 36.6 to 40.9% [35,36].

Here we present our results of the adsorption of (3-mercaptopropyl)trimethoxysilane (MPS) on iodine coated gold electrodes (Au–I). We study the adsorption of the MPS from alcoholic solution on Au(111)–I electrodes using atomic force microscopy (AFM) and X-ray photoelectron spectroscopy (XPS). We also study the adsorption of the MPS on polycrystalline iodine coated gold electrodes following reaction (1), and probe the defect sizes by studying the under potential deposition (upd) of lead on this modified electrodes. We compare our results with the adsorption of MPS on bare gold surfaces, both from alcoholic solution and electrochemical monolayer formation. Finally, we propose a scheme for the preparation of composite monolayers for molecular recognition experiments.

2. Experimental

Single gold electrodes, used in the AFM and XPS measurements, were prepared by heating and annealing vapor deposited gold over a chromium/crystal substrate in a H_2+O_2 flame. The electrodes were placed in a 1 mM KI solution for 5 min, and then washed with nanopure water and with EtOH. This produces a Au(111) iodine coated electrode surface (Au(111)–I) [29]. Then the Au(111)–I surfaces were placed in a 1 mM MPS in EtOH solution for 12 h before the analysis. This produced the MPS modified iodine coated gold surface (Au(111)–(MPS/I)). The MPS-SAM modified gold electrodes (Au(111)–MPS) used for the AFM analyses were formed by placing the bare Au(111) electrodes in a 1 mM MPS in EtOH solution for 12 h. The polycrystalline gold electrodes used for the electrochemical measurements were prepared by polishing a 0.5 mm diameter gold wire sealed in a glass tube with 1.0, 0.3, and 0.05 μm Al_2O_3 paste, and then rinsing copiously with nanopure water. After measurements the electrodes were cleaned in piranha solution for 1 min (3:1 conc. H_2SO_4/30% H_2O_2 solution, CAUTION: this solution reacts violently with organics). Then electrode cleanliness was verified by cycling the potential in a 0.1 M $HClO_4$ solution between the hydrogen and oxygen regions until characteristic CVs were observed. Then the electrode was polished with Al_2O_3 paste again, and washed copiously with nanopure water. The electrochemically active area of the electrodes was determined, employing the method described elsewhere [31], in a 0.1 M $HClO_4$ solution. The electrochemical cell employed was a conventional three-electrode cell using Pt gauze as a counter electrode. All potentials are reported with respect to the Ag | AgCl | 3 M NaCl reference electrode.

3. Results and discussion

3.1. Atomic force microscopy and X-ray photoelectron spectroscopy results of the MPS adsorption on Au(111)–I

AFM and XPS were used to characterize the modified Au surfaces. Examples of the MPS-SAM on Au(111) and Au(111)–I analyzed by AFM are shown in Figs. 1 and 2. The AFM images of the Au(111)–MPS surface show the complete coverage of the MPS-SAM over the grain boundaries of the (111) surface and the formation of porous structures (see Fig. 1). A line structure of the MPS-SAM is observed with line spacing of 2–3 nm, which is in accordance with previous work from our laboratory [37]. These results confirm that MPS forms a highly ordered monolayer on Au surfaces [20,21]. In contrast, AFM micrographs of the Au(111)–(MPS/I) surface shows a partial coverage of the MPS (see Fig. 2A). Comparing Fig. 2A and B with Fig. 1, in Fig. 2A and B the underlying (111) 60° structure is seen. The MPS tends to form clusters preferentially on the step edges, and partial coverage on the flat terraces (see Fig. 2B). The MPS forms a monolayer that extends over the terraces, and forms a cluster line structure with 6–10 nm line spacing (see Fig. 2C).

The MPS modified and unmodified Au(111)–I surfaces were studied by XPS. The XPS results of the Au(111)–(MPS/I), in the C (1s) binding energy region shows two peaks, one at 284 eV due to the methylene carbons in the MPS propyl chain, and another peak at 286 eV corresponding to the methyl carbons in the trimethoxy head (see Fig. 3A). The XPS peak, at the O

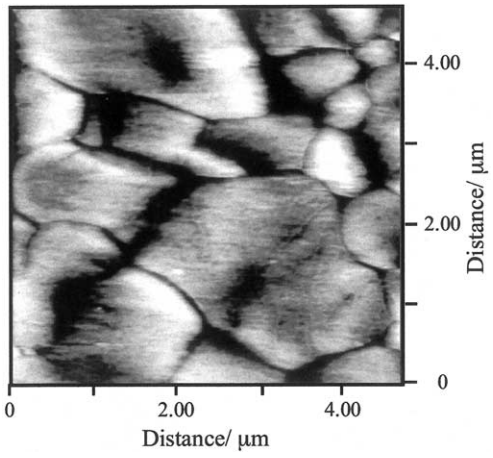

Fig. 1. AFM images of the MPS modified Au(111) at (5 × 5) μm magnification.

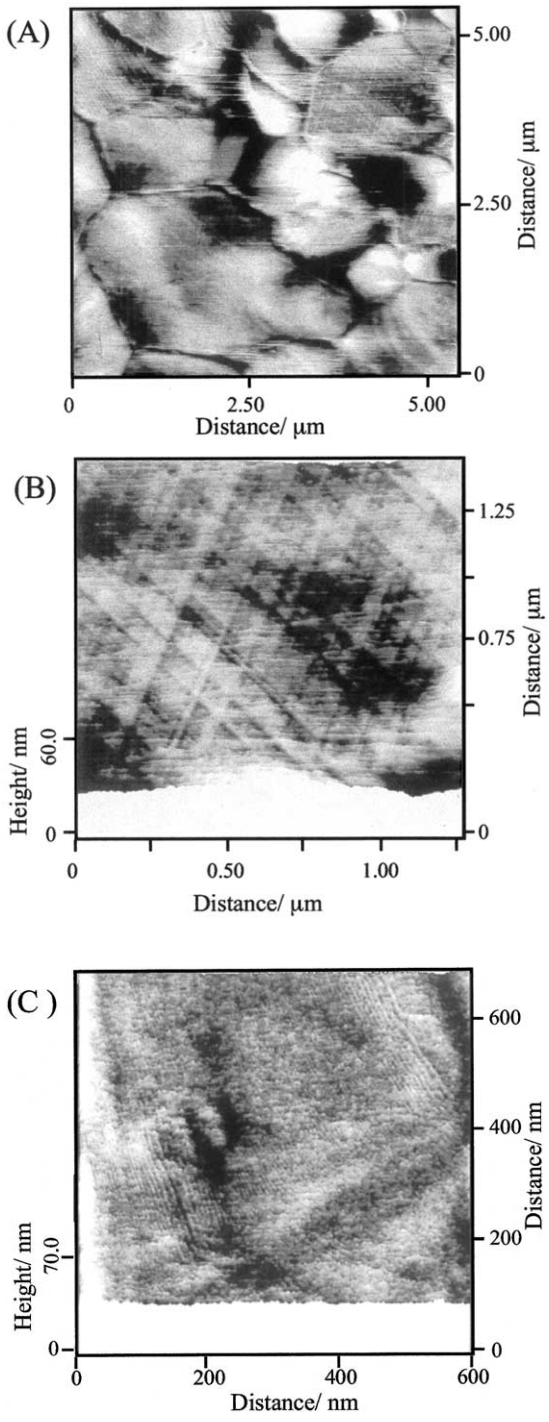

Fig. 2. Atomic force microscope images of the MPS modified iodine coated Au(111) electrode at: (A) low (5.25×5.25 μm); (B) high (1.25×1.25 μm); and (C) (600×650 nm) magnification. Partial surface coverage by MPS is seen in (A) and partial coverage of the flat terraces is seen in (B). A MPS line structure that continues over terraces with 6–10 nm line spacing is observed in (C).

(1s) binding energy region, increases in the Au(111)–(MPS/I) in comparison with the XPS of the unmodified Au(111)–I sample. The increase in the peak area corresponds to the oxygen present at the methoxy head group of the MPS molecule (see Fig. 3B). Fig. 4

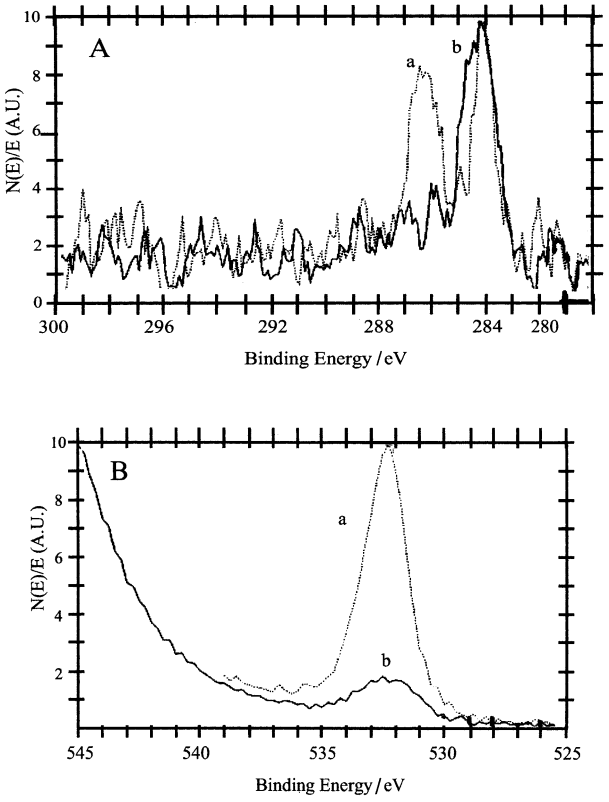

Fig. 3. X-ray photoelectron spectra for the (A) C (1s) and (B) O (1s) binding energy region for modified: (a) MPS–iodine coated gold electrode (dashed line); and (b) unmodified iodine coated gold electrode (solid line). Angle 45°, pass energy 5.8 eV for (A), and 58 eV for (B), Al monochromated source.

shows the principal I (3d) XPS binding energy region. The formation of an iodine zero-valent monolayer at 618.5 eV (see Fig. 4A(a)) for Au(111)–I interaction is observed. The Au(111)–(MPS/I) interaction was observed in Fig. 4B, which shows the presence of two iodine species. The curve fitting of the principal I (3d) XPS peaks shows one at 618.5 eV, similar to Fig. 4A(a) (see Fig. 4B(a)), and one at 618.9 eV signal (see Fig. 4B(b)), attributable to MPS/I interaction. This means that the chemical state of the iodine on the Au(111)–(MPS/I) surface is not the same as in Au(111)–I. In Fig. 4A(b) there is a small decrease on the iodine XPS signal observed for the Au(111)–(MPS/I) surface, due to the partial iodine desorption after MPS adsorption. Finally, two peaks are observed in the S (2p) binding energy region, at 161.8 and 163.0 eV (see Fig. 4C). The curve fit of S ($2p_{3/2}$) XPS peak reveals the presence of two sulfur species, one at 161.6 and 162.0 eV. The presence of sulfur peaks at 161.6 and 162.0 eV are characteristic of a gold thiolate bond [21,38]. The presence of the peaks can be explained in terms of the formation of MPS domains, with defects sites covered with iodine. The sulfur atoms inside the domains will give a higher binding energy, and those in the vicinity will give a lower binding energy.

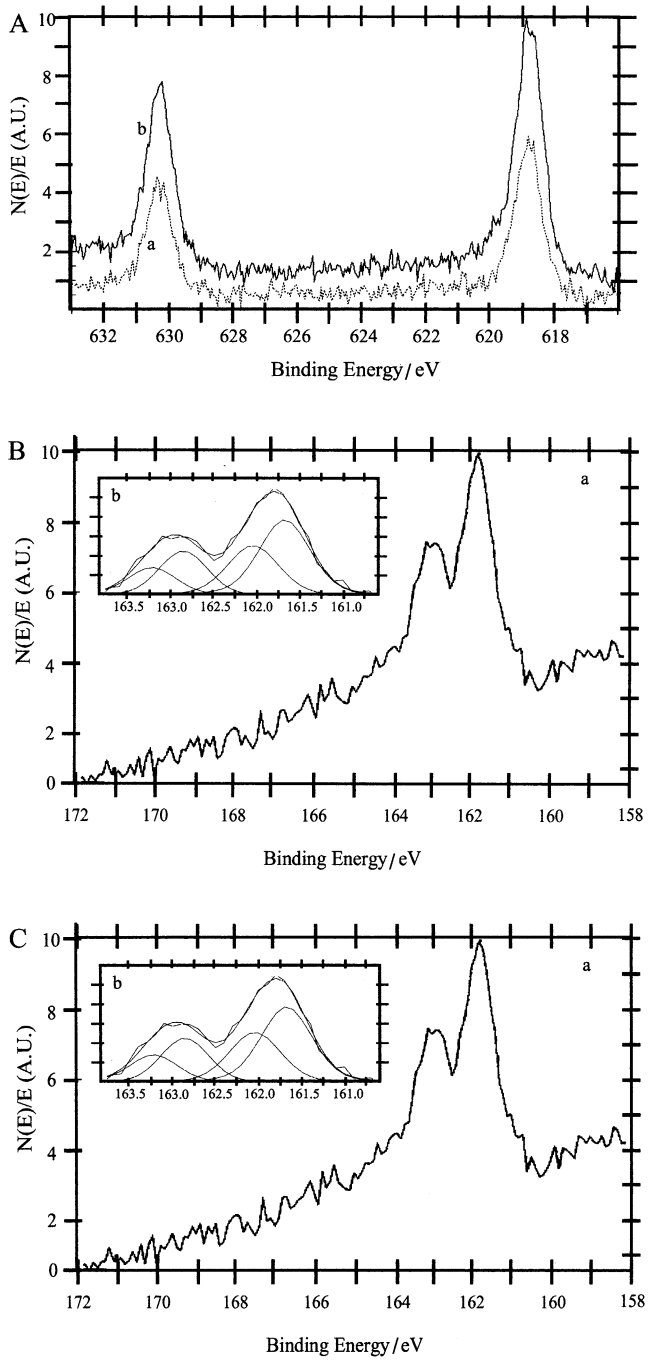

Fig. 4. X-ray photoelectron spectra for the (A) I (3d) binding energy region for modified: (a) MPS–iodine coated gold electrode (dashed line); and (b) unmodified iodine coated gold electrode (solid line). (B) X-ray photoelectron spectra for the S (2p) binding energy region for: (a) modified MPS–iodine coated gold electrode; and (b) curve fit. Angle 45°, pass energy 5.8 eV for (A), and 11.75 eV for (B), Al monochromated source.

The atomic concentrations were in accordance with MPS adsorbed on the Au(111)–I surface. From the atomic concentrations we establish an approximate S/I ratio of 2 to 1. A graph showing how the atomic concentration for Au, C, O, Si, S and I varies as a function of the angle (with respect to the surface normal) of the photoelectron detection is shown in Fig. 5. These results confirm that the sulfur and iodine atoms are closer to the Au surface (i.e. bounded to the gold surface), while oxygen and silicon are detected away from the surface (i.e. they are part of the thiol head). The gold binding energy peak diminishes at larger angles (film | air interface), as is expected, which confirms the veracity of the method used.

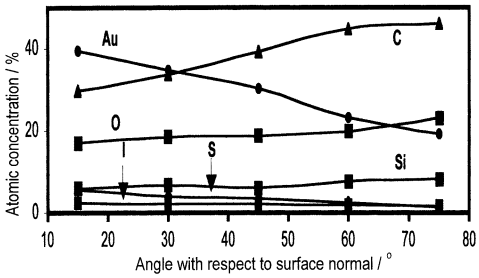

Fig. 5. X-ray photoelectron angle resolved measurements for the modified MPS–iodine coated gold electrode. The figure presents a plot of atomic concentration percent vs. angle of detection with respect to the surface normal. All elements are included.

It is clear from the AFM results that the iodine monolayer prevents the self-assembly process of the MPS producing a low-density package monolayer with spacing larger than that of the Au–MPS. These results are different from our previous work with MPS on gold [29]. The lower coverage of the MPS on the iodine coated electrodes, and the ordered structures observed, could be explained if the MPS partially displaces the iodine from the surface. This creates MPS domains, in which the sulfur head bonds directly to the gold surface in the positions from which iodine has been displaced. This leaves the iodine adlayer intact on the thiol free regions, producing a composite monolayer where the defect sites are covered with iodine (Au–(MPS/I)). This may explain why the iodine species present on the MPS-SAM modified surfaces are equivalent to that in unmodified iodine coated gold electrodes from the XPS results. The sulfur binding energy is consistent with a Au–S bond. According to Fig. 4A, the XPS spectra Fig. 4A(a), presents less iodine on gold than that of the Au(111)–I surface seen in Fig. 4A(b). This is in agreement with the MPS displacement of iodine from the Au surface and a decrease in the iodine–gold coverage. From these results we can state a reaction analog to that proposed by Soriaga et al., for the thiol adsorption on Pt–I [39]:

$$\mathrm{Au{-}I_{(ads)}} + \mathrm{MPS{-}H_{(EtOH)}} \leftrightarrow \mathrm{Au{-}MPS_{(ads)}} + \mathrm{H^{+}_{(EtOH)}} + \mathrm{I^{-}_{(EtOH)}} \quad (2)$$

On the other hand, our results are different from that observed by Batina and coworkers for the self-assembly of organic molecules over iodine coated gold electrodes,

in which the molecular adlayers are formed over the iodine monolayer [29,30].

3.2. Electrochemically formed MPS monolayers

The MPS monolayers on gold surfaces were formed electrochemically using reaction (1) and the procedure presented in Refs. [26–28]. Fig. 6A shows the cyclic voltammograms of polycrystalline gold in 0.1 M KCl and 1 mM MPS aqueous solution. The initial potential was held at 0.120 V for 30 s prior to the negative potential sweep. More adsorption of the MPS is achieved at this initial potential; therefore, a monolayer with smaller defect sizes is obtained by cycling the potential between 0.120 and −1.20 V. After several potential scans the electrode surface becomes passivated because of the electrochemical polymerization of the MPS monolayer [26,27]. In Fig. 6C we can observe the reductive-desorption and oxidative-adsorption of iodine on polycrystalline gold electrodes in 0.1 M KCl and 1 mM KI solution. This CV is similar to that observed by Rodriguez and Soriaga in which they use thin layer

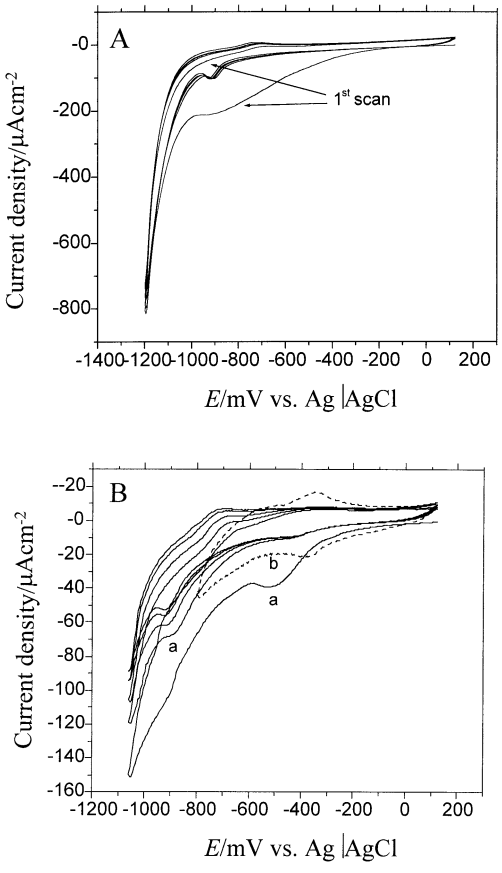

Fig. 6. Cyclic voltammetry of polycrystalline gold electrode in: (A) 0.1 M KCl+1 mM MPS solution; (B) (a) 0.1 M KCl+1 mM KI+1 mM MPS solution (solid line); and (b) 0.1 M KCl+1 mM KI solution (dashed line) at a scan rate of 200 mV s^{-1}. All data are presented from the first scan. The initial potential was held for 30 s before the negative potential sweep was recorded.

cyclic voltammetry in 1 M $NaClO_4$ electrolyte solution in the absence of iodine [40]. Fig. 6B corresponds to the electrochemical adsorption of the MPS molecule on an iodine-coated gold electrode using a 0.1 M KCl+1 mM MPS+1 mM KI solution. Note that after the first scan the behavior is the same as that presented in Fig. 6A. The broad peak observed in Fig. 6B at −0.350 to −0.700 V versus Ag | AgCl, during the first scan, consists of two peaks. These are due to the partial irreversible desorption of the iodine adlayer followed by the desorption of the MPS monolayer formed at the initial potential. The reductive desorption peak of iodine is shifted to more negative potentials due to the MPS adsorption. The cathodic peaks observed around −0.900 V, after the first scan for the Au–MPS and Au–(MPS/I), are due to the MPS desorption, and the anodic peaks observed around −0.700 V are due to the MPS adsorption. Also, it can be observed that as the number of scans increases the MPS desorption peak is shifted toward a more negative potential value for both samples. This is due to the formation of a monolayer with few defects and to the MPS polymerization at the surface (see Fig. 6). The polymerization of the MPS on Au and Cu surfaces proceeds through the loss of the methoxy groups, and the formation of –Si–O–Si– bonds between MPS neighbor molecules, the polymers also have –Si–OH defects [20,21,26–28,37,41,42]. If the mechanism of MPS adsorption during the initial potential deposition is the same as that in ethanolic solution, then we can describe the electrochemical formation process of the Au–(MPS/I) composite surface with the following electrochemical reaction:

$$\mathrm{Au{-}I_{(ads)} + MPS{-}H_{(ac)} + e^-} \leftrightarrow \mathrm{Au{-}MPS_{(ads)} + H^+_{(ac)} + I^-_{(ac)}} \quad (3)$$

This electrochemical displacement reaction between the iodine and the MPS can be used to control the defect sizes by controlling the initial potential and/or the number of cycles between the initial potential and −1.06 V in 0.1 M KCl+1 mM MPS+1 mM KI solution. By varying the equilibrium of Eq. (3) to the right, we can produce a thiol monolayer with smaller defect sites (i.e. less iodine). In this work, we probe the composite monolayer defects prepared with different numbers of cycles, by observing the electrochemical deposition of Pb. The degree of penetration of the Pb^{2+} gives an indication of the defect sizes of the surface; this procedure has been employed to evaluate the defect structure of MPS-SAM-modified electrodes [20]. Zeng and Bruckenstein have shown recently that upd of Pb^{2+} on gold electrodes, from supporting electrolytes containing chloride and nitrate ions follows the reduction of free lead ions from solution, and from the reduction of adsorbed lead chloride complex with stoichiometry $PbCl_4^{2-}$ [43,44]. They showed that at positive potentials,

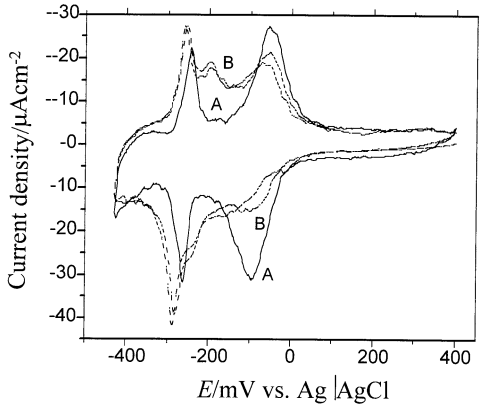

Fig. 7. Cyclic voltammetry of the lead underpotential deposition (upd) on (A) bare polycrystalline gold electrode (solid line), and (B) iodine modified gold electrode (dashed line) from a 0.1 M KCl+10^{-4} M HCl+1 mM $Pb(NO_3)_2$ solution, at a scan rate of 50 mV s^{-1}.

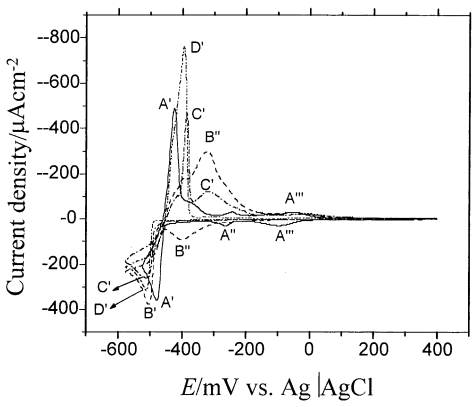

Fig. 8. Cyclic voltammetry of lead deposition on modified Au–(MPS/I) electrodes prepared by different numbers of cycles (according to Eq. (3)): (A) unmodified gold electrode; (B) 30 s at initial potential, 0 cycles; (C) one cycle; and (D) five cycles in 0.1 M KCl+1 mM KI+1 mM MPS solution, at a scan rate of 200 mV s^{-1}. The lead deposition was made from a 0.1 M KCl+10^{-4} M HCl+1 mM $Pb(NO_3)_2$ solution, at a scan rate of 50 mV s^{-1}. The first potential cycle is presented for each case.

adsorbed chloride promotes the formation of the lead complex; the resulting cyclic voltammetry of lead upd is shown in Fig. 7A. Two peaks for the underpotential deposition of lead on bare gold electrodes are observed at −0.082 and −0.260 V. The resulting cyclic voltammogram for the underpotential deposition of lead on iodine coated gold electrodes is presented in Fig. 7B; two cycles are presented. In this case three peaks are observed during the first cycle of deposition, a small shoulder at −0.082 V, another small shoulder at −0.250 V, and, during the second and third cycle, two peaks are observed, at −0.082 and −0.254 V, and a peak at 0.290 V, comparable with Fig. 6C. In the lead anodic stripping step two peaks are observed for the bare gold, and three are observed for the iodine coated gold electrode. This behavior during the lead deposition is expected, since the iodine monolayer blocks the gold surface, preventing the formation of the lead chloride complex; nevertheless the lead deposition is achieved at a 40 mV overpotential. We have observed that after several scans (i.e. more than 10), the cyclic voltammogram for Au–I resembles the lead upd on bare gold. This may be due to the complete or partial loss of iodine during the lead deposition/dissolution cycles.

The electrodeposition of Pb was done on the MPS modified Au–I surfaces. A comparison was done with bare Au electrodes. Fig. 8A shows the cyclic voltammetry for the lead deposition on bare gold, showing the bulk and upd regions. In the figure peak A′ is due the lead bulk deposition at −0.460 V, and peaks A″ and A‴ are the upd peaks shown in Fig. 7A. Fig. 8(B–C) shows the cyclic voltammetry for the lead deposition for the modified Au–(MPS/I) electrodes prepared according to Eq. (3), i.e. varying the surface modification conditions electrochemically in 0.1 M KCl+1 mM KI+1 mM MPS solution. The first Au–(MPS/I) surface, sample B, was prepared as follows. A Au–I electrode was placed in the MPS solution described above, for 30 s at 0.120 V, without sweeping the potential (see Fig. 8B). The surface modification conditions for the other Au–(MPS/I) surfaces were as follows, the Au–I electrodes were placed in the MPS solution for 30 s at 0.120 V initial potential, afterwards the potential was swept between 0.120 and −1.060 V, with different cycling times, at a scan rate of 200 mV s^{-1}. The number of cycles between the potential ranges was one for sample C (Fig. 8C) and five for sample D (Fig. 8D). From the observed cathodic peaks it can be said that the only sample presenting a upd peak is the one prepared by holding the initial potential for 30 s, in the MPS solution and applying no potential cycles (sample B). This Au–(MPS/I) surface exhibits a broad upd peak at −0.400 V (peak B″ in Fig. 8B), more negative than peak A″ for the bare Au electrode, and the peaks observed for Au–I electrode in Fig. 7B. Also the lead bulk deposition peak potential is shifted toward a more negative value (peak B′). This confirms that at the initial potential the MPS adsorption takes place, partially displacing the iodine monolayer. As the potential is cycled, the Pb upd peaks disappear and the Pb bulk deposition peak shifts toward a more negative potential value as the number of potential scans is increased. By observing the lead stripping peaks we can observe that even when the Au–(MPS/I) surface is prepared with one cycle in the MPS solution (sample C), the upd peak is not present. The Pb stripping peak for this Au–(MPS/I) electrode (peak C′ in Fig. 8C) is similar to that of sample B (peak B″ in Fig. 8B). The only difference is that peak B″ appears as a broad peak between −0.200 and −0.350 V with a small shoulder at −0.390 V, and peak C′ has a well defined peak at that potential and a broad peak between −0.200 and −0.350 V (see Fig. 8B and C). Moreover, we can observe that both samples B and C, present an anodic peak in the

same region as peak A‴, which in bare gold is due to the lead dissolution formed at upd. This is not the case for the Au–(MPS/I) electrode prepared by sweeping the potential above five cycles between the potential limits presented above. In the MPS solution (sample D, Fig. 8D), only one anodic peak is observed at around −0.400 V (peak D′). From these results it can be demonstrated that by increasing the number of cycles during the preparation of the Au–(MPS/I) surface, the permeability of the lead ions through the MPS/I adlayer decreases. This can be explained by displacing the equilibrium described by Eq. (3) to the right, forming a thiol/iodine composite monolayer with smaller defect sites.

4. Conclusions

As a concluding remark we propose a scheme for the preparation of composite monolayer modified electrodes for molecular recognition experiments. The key part in this proposed procedure is to control the amount of iodine on the Au surface electrochemically. In this way the amount of MPS can be controlled indirectly. First the iodine adlayer is formed upon adsorption from KI solution. The amount of iodine on the surface can be controlled by anodic stripping in $HClO_4$ solution. The partially iodine-coated electrode is transferred to an alcoholic MPS solution for the MPS adsorption. Afterward this electrode can be placed in water for the MPS polymerization. The electrochemical adsorption of the MPS under the same conditions as in Fig. 6B can be used for the composite monolayer preparation. The amount of iodine can be reduced (i.e. by increasing the amount of MPS) by cycling the potential between the initial and the iodine desorption potential. We have found that due to the presence of MPS, this potential is shifted toward a more negative potential (see Fig. 6B). By varying the number of cycles between the initial and the MPS desorption potential the defect sizes of this composite monolayer can be controlled, as is shown from lead electrodeposition results (see Fig. 8). The Au–(MPS/I) composite monolayer can be employed to produce nanostructures.

Acknowledgements

The authors would like to acknowledge the financial support of NSF-ESPCoR grant number HER-9108775 and OSR-9452893, NSF graduate fellowship, and the NIH-MARC Program. The use of the Surface Microscopy and Spectroscopy Facility of the Materials Characterization Research and Services Center at the University of Puerto Rico is gratefully acknowledged. The help given by Professor Raul J. Castro (UPR at Cayey) and Dr. Esteban Fachini (UPR-Río Piedras) during some of the XPS measurements is also acknowledged.

References

[1] A. Ulman, An Introduction to Ultrathin Organic Films from Langmuir-Blodgett to Self-Assembly, Academic Press, New York, 1991.
[2] E.L. Smith, M.D. Porter, J. Phys. Chem. 97 (1993) 8032.
[3] J.D. Swalen, D.L. Allara, J.D. Andrade, E.A. Chandross, S. Garoff, J. Isreaelachvilli, T.J. McCartthy, R. Murray, R.F. Pease, J.F. Rabolt, K.J. Wynne, H. Yu, Langmuir 3 (1987) 932.
[4] L. Tender, M.T. Carter, R. Murray, Anal. Chem. 66 (1994) 3173.
[5] C.D. Bain, G.W. Whitesides, Angew. Chem., Int. Ed. Engl. 28 (1989) 506.
[6] G.W. Whitesides, P.E. Laibinis, Langmuir 6 (1990) 87.
[7] V. De Palma, N. Tillman, Langmuir 5 (1989) 868.
[8] M.P. Soriaga, A.T. Hubbard, J. Am. Chem. Soc. 104 (1982) 3937.
[9] R.W. Murray, Acc. Chem. Res. 13 (1980) 135.
[10] H.O. Finklea, M.S. Ravenscroft, D.A. Snider, Langmuir 9 (1993) 223.
[11] C. Miller, P. Cuendet, M. Gratzel, J. Phys. Chem. 95 (1991) 877.
[12] C.E.D. Chidsey, Science 251 (1991) 919.
[13] L. Sun, B. Johnson, T. Wade, R.M. Crooks, J. Phys. Chem. 94 (1990) 8869.
[14] M. Kunitake, K. Akiyoshi, K. Kawatana, N. Nakashima, O. Manabe, J. Electroanal. Chem. 292 (1990) 227.
[15] A.M. Becha, C.J. Miller, J. Phys. Chem. 96 (1992) 2657.
[16] C. Miller, M. Gratzel, J. Phys. Chem. 95 (1991) 5225.
[17] W.R. Everett, T.L. Welch, L. Reed, I. Frich-Faules, Anal. Chem. 67 (1995) 292.
[18] M.D. Porter, T.B. Bright, D.L. Allara, C.E.D. Chidsey, J. Am. Chem. Soc. 109 (1987) 3559.
[19] J.D. Tirado, D. Acevedo, R.L. Bretz, H. Abruña, Langmuir 10 (1994) 1971.
[20] W.R. Thompson, M. Cai, M. Ho, J.E. Pemberton, Langmuir 13 (1997) 2291.
[21] J. García-Orozco, M.A. Thesis, University of Puerto Rico, Puerto Rico, 1997.
[22] C.A. Widrig, C. Chung, M.D. Porter, J. Electroanal. Chem. 310 (1991) 335.
[23] M.M. Walczak, D.D. Poperoe, P.R. Deinhammer, B.D. Lamp, C. Chung, M.D. Porter, J. Am. Chem. Soc. 114 (1992) 5860.
[24] M.M. Walczak, D.D. Poperoe, P.R. Deinhammer, B.D. Lamp, C. Chung, M.D. Porter, Langmuir 7 (1991) 2687.
[25] T.W. Schneider, D.A. Buttry, J. Am. Chem. Soc. 115 (1993) 12391.
[26] G. Che, C.R. Cabrera, J. Electroanal. Chem. 417 (1996) 155.
[27] G. Che, A. Manivannan, C.R. Cabrera, C.R. Physica A 231 (1996) 304.
[28] G. Che, H. Zhang, Z. Li, C.R. Cabrera, J. Electroanal. Chem. 437 (1997) 13.
[29] M. Kunitake, N. Batina, K. Ogaki, Y.G. Kim, L.J. Wan, T. Yamada, K. Itaya, Solid–Liquid Electrochemical Interfaces; ACS symposium series 656, 1997, p. 171.
[30] M. Kunitake, N. Batina, K. Itaya, Langmuir 11 (1995) 2337.
[31] J.F. Rodriguez, T. Mebrahtu, M.P. Soriaga, J. Electroanal. Chem. 233 (1987) 283.
[32] R.L. McCarley, A.J. Bard, J. Phys. Chem. 95 (1991) 9618.
[33] X. Gao, M.J. Weaver, J. Am. Chem. Soc. 114 (1992) 8544.
[34] N.J. Tao, S.M. Lindsay, J. Phys. Chem. 96 (1992) 5213.
[35] N. Batina, T. Yamada, K. Itaya, Langmuir 11 (1995) 4568.

[36] B.M. Ocko, G.M. Watson, J. Wang, J. Phys. Chem. 98 (1994) 897.
[37] A. Morneau, A. Manivannan, C.R. Cabrera, Langmuir 10 (1994) 3940.
[38] T. Ishida, M. Hara, I. Kojima, S. Tsuneda, N. Nishida, H. Sasabe, W. Knoll, Langmuir 14 (1998) 2092.
[39] M.P. Soriaga, G.M. Berry, E. Binamira-Soriaga, Colloids Surf., A 134 (1998) 31.
[40] J.F. Rodriguez, M.P. Soriaga, J. Electrochem. Soc. 135 (1988) 616.
[41] R.J. Tremont, H. De Jesus-Cardona, J. Garcia-Orozco, R.J. Castro, C.R. Cabrera, J. Appl. Electrochem. 30 (2000) 737.
[42] R.J. Tremont, C.R. Cabrera, J. Appl. Electrochem. 32 (2002) 783.
[43] X. Zeng, S. Bruckenstein, J. Electrochem. Soc. 146 (1999) 2549.
[44] X. Zeng, S. Bruckenstein, J. Electrochem. Soc. 146 (1999) 2555.